Turbulent Flow Through Pipe

SmartNumerics Simulation Solutions Inc.

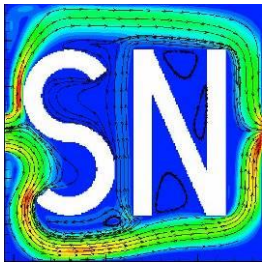

June 8, 2020

This study is not a validation document but may be of interest. As related by Patel [1], velocity in smooth pipes typically shows a peak in centerline velocity at about 40 pipe diameters. Klein [2] indicates that the location of the peak velocity may range from 35 to 40 pipe diameters. This peak is as much as 4% larger than the fully developed value. Downstream of the peak, the centerline velocity then decays to the fully developed value. This complex behaviour is thought to be due to interaction of boundary layers from opposite sides of the pipe as they merge.

Reichert and Azad [3] have performed experiments involving turbulent flow of air through a pipe for values of

$$\mathrm{Re}_R = \frac{\rho_{\mathrm{ref}} R}{\mu_{\mathrm{ref}}} U_{\mathrm{avg}}$$

ranging from 5.6×10^4 to 1.53×10^5. Here R is the pipe radius, ρ_{ref} is the reference density, μ_{ref} is the reference molecular viscosity, and U_{avg} is the bulk (cross-section averaged) velocity. They give the approximate peak position as a function of Re_R as

$$\frac{x_p}{D} = 30.80 + \frac{0.89}{\mathrm{Re}_R \; x \; 10^{-5}} + \frac{0.79}{\left(\mathrm{Re}_R \; x \; 10^{-5}\right)^2} \quad .$$

This formula places the peak at 34.9 pipe diameters for Re_R equal to 5.6×10^4 and at 31.7 at Re_R equal to 1.53×10^5. Simulations based on these experiments have been performed by Wang [4] and Kumara, Halvorsen, and Melaaen [5].

The experiments were performed in a fully developed pipe flow wind tunnel described in Azad and Hummel [6] and Ozimek [7]. This wind tunnel uses a fan to drive air at standard atmospheric conditions though a contraction nozzle which connects to the leading edge of the pipe. The contraction nozzle reduces the flow area by a factor of 89 and increases the flow speed by the same factor. The tunnel can produce velocities of 15 to 75 m/s in the pipe. The atmospheric pressure in the laboratory varies from 730 mm of Hg (97325.3 Pascals) to 750 mm of Hg (99991.8 Pascals) and the temperature varies from 22°C to 28°C with 23°C to 25°C being most common. Setting the pressure to 99,710 Pascals, the temperature to 24.2°K, and the flow speed to 17.3 m/s gives a Reynolds number equal to 5.6×10^4. The density is 1.168 kg/m^3 and the Mach number is 0.05. Using the Sutherland formula for molecular viscosity, the corresponding kinematic viscosity is 1.57×10^{-5} m^2/s.

According to Ozimek [7], for a flow speed of 8 m/s in the pipe, the longitudinal turbulent intensity decreases from 30% at the mouth of the contraction nozzle to approximately 0.45% at the outlet of the

contraction nozzle. The flow speed increases from about 0.09 m/s at mouth of the contraction nozzle to 8 m/s at the outlet while the velocity fluctuations decrease in magnitude as the gas approaches the outlet.

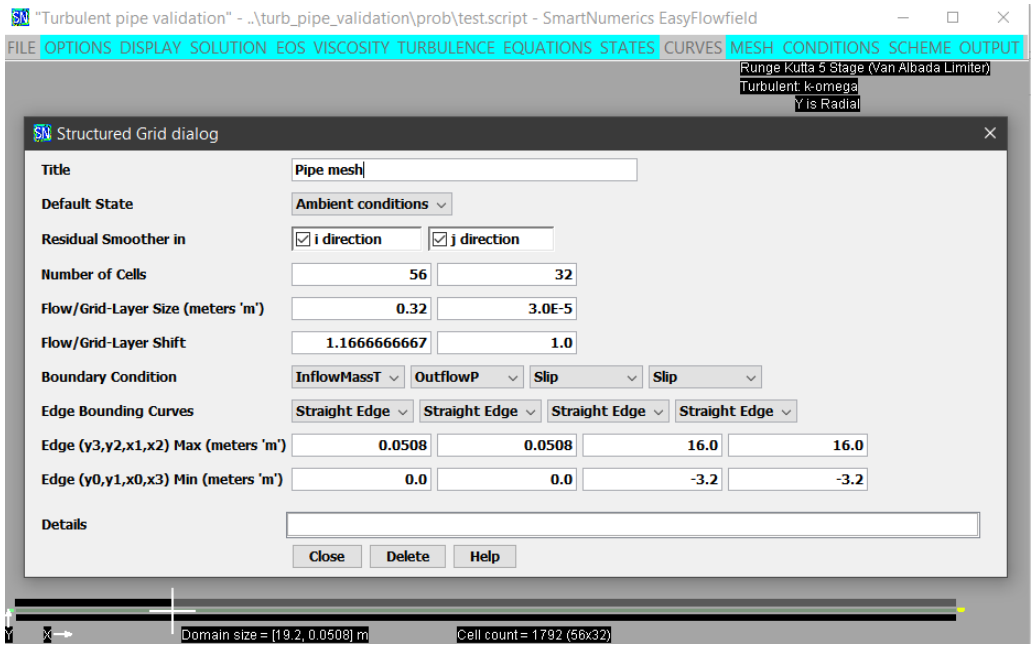

Fig. 1: Grid and k-ω turbulence model input for turbulent flow over flat plate.

Figure 1 displays the dialog used to generate a grid for simulation of turbulent flow of air (ideal-gas equation of state) through a smooth walled pipe. The no-slip wall (grey) boundary is imposed using an additional dialog. The k-ω turbulence model of Wilcox [8] is used without a wall function. The initial and inflow-reference conditions are 17.3 m/s, 101150 Pascals, and 24.2° C. A static pressure of 99,710 Pascals is imposed at the outlet. An inflow condition with fixed mass flow and total temperature is imposed on the left. The inflow turbulence intensity was set to 0.45% and the inflow eddy viscosity was one tenth of the molecular viscosity. The simulation was solved using an explicit five stage Runge-Kutta solver with enriched w-cycle multigrid. The HLLC flux was used with the van Albada limiter.

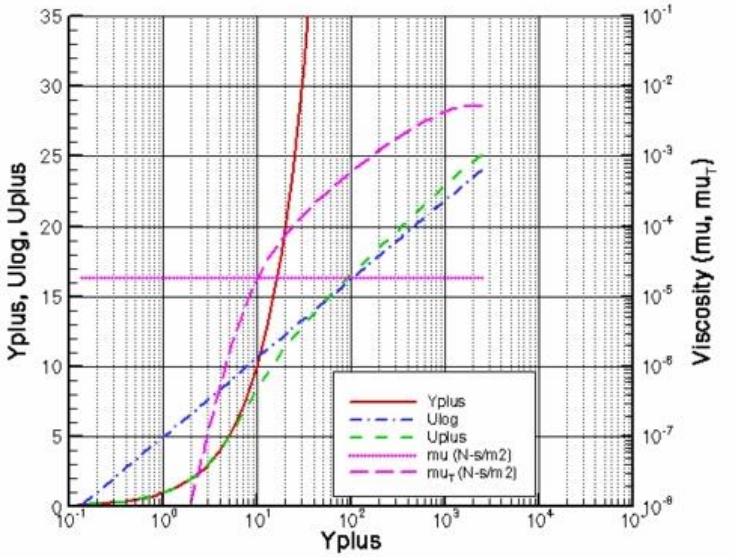

Fig. 2: Plot of viscosity and u^+ versus y^+ for turbulent flow through smooth pipe.

Figure 2 displays a comparison of $u^+ = u/u^*$ to the incompressible log law

$$U_{\log} = \frac{1}{0.41}\ln\left(y^+\right) + 5.0$$

at a region downstream of the leading edge. As expected, the u^+ curve conforms to the y^+ curve near the wall. Also shown is the variation of molecular viscosity and eddy viscosity.

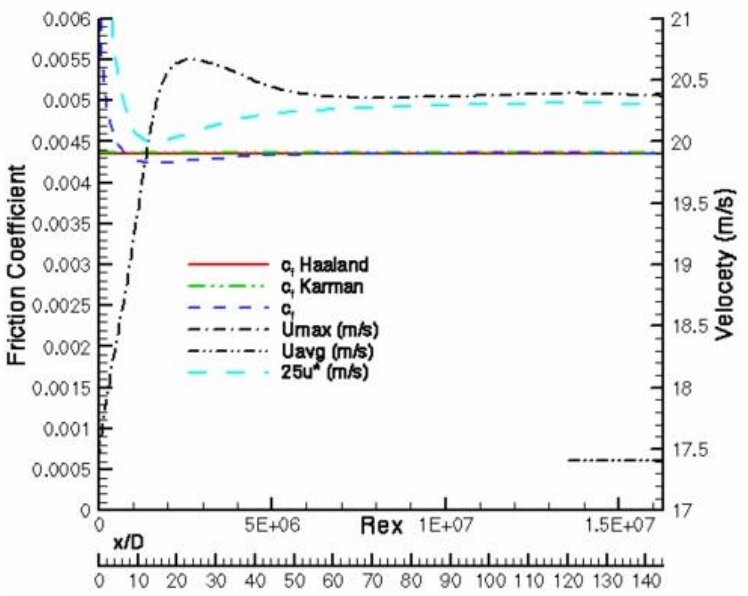

Fig 3: Plot of skin friction vs Reynolds number for flow through smooth pipe.

Figure 3 displays the skin friction along the pipe wall as a function of Reynolds number based on distance downstream from the leading edge. The skin friction coefficients are computed using

$$c_f = 2\frac{\rho_w\left(u^*\right)^2}{\rho_{\text{ref}}U_{\text{avg}}^2}$$

using the local friction velocity, u^*, output by the solver. Here, ρ_w is the local density at the wall, ρ_{ref} is the reference density which is generally set to the centerline density at the outlet, and U_{avg} is the velocity averaged over the outlet cross section.

Also plotted is the velocity along the center of the pipe ($U_{\max}$), the average velocity computed at the end of the pipe, and the friction velocity multiplied by 25. Here

$$\text{Re}_x = \frac{\rho_{ref}x}{\mu_{ref}}U_{\text{avg}}$$

is the Reynolds number a specified distance x downstream of the leading edge of the pipe. Note that the reference density is taken from the centerline at the outflow boundary and the bulk velocity is the average velocity at the outflow boundary. The compressible flow equations are being solved. Thus, the bulk velocity is slightly larger than the specified inflow velocity. The friction curve is a good fit to the friction correlations of von Karman and Haaland at the outflow boundary. The peak is at 23.4 pipe diameters.

The von Karman friction correlation for smooth pipes has the form

$$\frac{1}{\sqrt{4c_f}} = 1.74 - 2\log_{10}\left(\frac{18.6}{\mathrm{Re}_D\sqrt{4c_f}}\right)$$

where

$$\mathrm{Re}_D = \frac{\rho_{\mathrm{ref}} D}{\mu_{ref}} U_{\mathrm{avg}}$$

is the Reynolds number based on pipe diameter. This expression is solved in an iterative manner starting with an initial guess for C_f.

The friction correlation of Haaland [9] is defined as

$$\frac{1}{\sqrt{4C_f}} = -1.8\log_{10}\left(\left(\frac{d_{eq}}{3.7D}\right)^{1.11} + \frac{6.9}{\mathrm{Re}_D}\right)$$

where d_{eq} is the equivalent sand grain diameter or absolute roughness (a measure of wall roughness). Here d_{eq} is set to a value typical of smooth drawn tubing ($1.52\text{x}10^{-6}$ meters) tabulated for the pipe-flow diagrams based on the work of Moody [10].

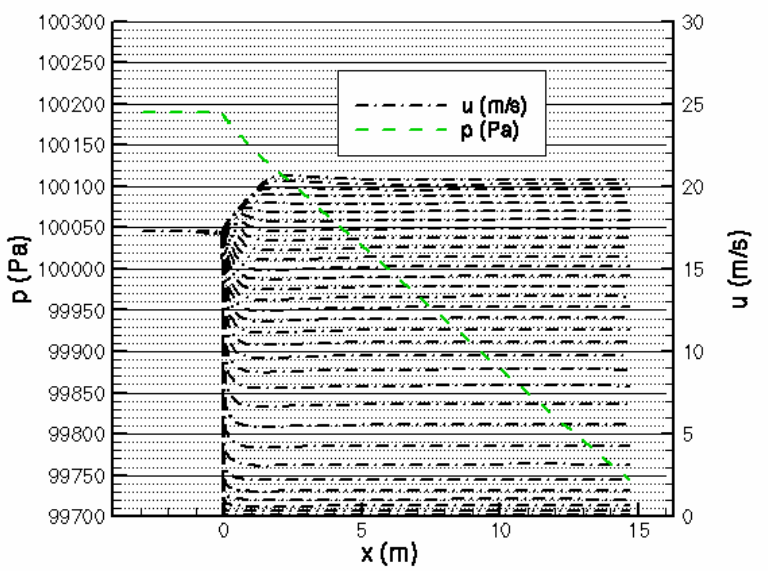

Fig 4: Pressure and velocity profiles for flow through smooth pipe.

Figure 4 displays the stream-wise variation of pressure upstream of and within the pipe. Also shown is the stream-wise flow velocity at various distances from the wall.

Table 1: Location (x/D) of peak centerline velocity for various values of inflow turbulence intensity.

Model	**5.8% Int.**	**1% Int.**	**0.45% Int.**	**0.1% Int.**	**0.01% Int.**
Std. k-ω	23.3	23.3	23.4	23.9	32.5
k-ω 2006	24.3	24.3	24.3	25.4	30.3

As also found by Wang [4] and Kumara, Halvorsen, and Melaaen [5], the peak obtained using simulation lies somewhat upstream of the experimental location. As shown in Table 1, the location of the peak moves downstream for small values of turbulence intensity. However, the peak becomes less pronounced.

The k-ω 2006 model of Wilcox [11] displays a higher peak velocity usually located further downstream than the k-ω model. The k-ω 2006 stress limiter weight was set to zero to prevent a disturbance upstream of the pipe mouth.

Note that for a given pipe length, diameter, inlet fluid density, and desired average flow speed, the pressure drop through a circular pipe with turbulent flow can be approximated by

$$p_{in} - p_{out} = -2\frac{L}{D} c_f \rho \left(U_{\text{avg}}\right)^2 \quad .$$

Thus, the pressure drop through a pipe of given length varies as the square of the average flow speed. Since gas is compressible, the centerline velocity at the outflow boundary will rise above the peak velocity for large enough values of average flow velocity.

Simulations of the flow of air or water through rough-walled pipes have been performed. The location of peak velocity moves further upstream as wall roughness is increased.

References

[1] Patel, B. R., "Internal Flows," in Fundamentals of Fluid Mechanics, Edited by Schetz, J. A. and Fuhs, A. E., John Wiley and Sons, New York, 1999.

[2] Klein, A. "Review: Turbulent developing pipe flow," Journal of Fluids Engineering, Vol. 103, p. 243-249, 1981.

[3] Reichert, J. K., Azad, R. S. "Nonasymptotic behaviour of developing turbulent flow," Canadian Journal of Physics, pp. 268-278, 1976.

[4] Wang, Y. Q., Prediction of Developing Turbulent Pipe Flow by a Modified K-ε-γ Model, PhD thesis, University of Manitoba, Winnipeg, Manitoba, 1999.

[5] Kumara, W. A. S., Halvorsen, B. M., Melaaen, M. C. "Computational study on non-asymptotic behaviour of developing turbulent pipe flow," Advances in Fluid Mechanics VIII, pp. 39-53, 2010.

[6] Azad, R. S., Hummel, R. H., "Measurement on the intermittency factor in diffuser-flow," Canadian Journal of Physics, Vol. 49, pp. 2917-2930, 1971.

[7] Ozimek, L. G., A Comparison of Analog and Digital Data for Measurements of Turbulence Parameters, MSc Thesis, University of Manitoba, Winnipeg, Manitoba, 1985.

[8] Wilcox, D. C., Turbulence Modeling for CFD, DCW Industries Inc., 1994.

[9] Haaland, S. E. "Simple and explicit formulas for the friction factor in turbulent flow", Trans. ASME, J. of Fluids Engineering, 103:89–90, 1983.

[10] Moody, L. F., "Friction Factors for Pipe Flow," Transactions of the ASME, November 1944.

[11] Wilcox, D. C., Turbulence Modeling for CFD, 3rd ed., DCW Industries Inc., 2006.